

Perturbative renormalization of GPDs to $O(a^2)$, for various fermion/gluon actions

Martha Constantinou*[†], Haralambos Panagopoulos, Fotos Stylianou[†]

Department of Physics, University of Cyprus,

P.O.Box 20537, Nicosia CY-1678, Cyprus

E-mail: marthac@ucy.ac.cy, haris@ucy.ac.cy, fstyli01@ucy.ac.cy

We present a 1-loop perturbative calculation of the fermion propagator, up to $\mathcal{O}(a^2)$ (a : lattice spacing). The fermions are described by Wilson, clover and twisted-mass actions; for gluons we use Symanzik improved actions (Plaquette, Tree-level Symanzik, Iwasaki, TILW, DBW2). Our results are given in a general covariant gauge, and their dependence on the coupling constant, the external momentum, the masses and the clover parameter is shown explicitly. We also study the $\mathcal{O}(a^2)$ corrections to matrix elements of unpolarized/polarized fermion bilinear operators, which include up to one derivative. These corrections are essential ingredients for improving, to $\mathcal{O}(a^2)$, the renormalization constants of the operators under study. In addition, they can be used to minimize lattice artifacts in non-perturbative studies.

PACS: 11.15.Ha, 12.38.Gc, 11.10.Gh, 12.38.Bx

*The XXVII International Symposium on Lattice Field Theory
July 26-31, 2009
Beijing, China*

*Speaker.

[†]Work supported in part by the Research Promotion Foundation of Cyprus (Proposal Nr: TEXN/0308/17)

1. Introduction

A major issue of Lattice Gauge Theory has been the reduction of effects which are due to the finite lattice spacing a , in order to better approach the elusive continuum limit. Over the years, many efforts have been made for $\mathcal{O}(a^1)$ improvement in lattice observables, which in many cases is automatic by virtue of symmetries of the fermion action. According to Symanzik's program [1], one can improve the action by a judicious addition of irrelevant operators. Also, in the twisted mass formulation of QCD [2] at maximal twist, certain observables are $\mathcal{O}(a^1)$ improved, by symmetry considerations. The first 1-loop perturbative computation of $\mathcal{O}(a^2)$ effects was recently performed by our group [3]. This regards the evaluation of the fermion propagator and Green's functions for ultralocal bilinears of the form $\mathcal{O}_\alpha^\Gamma = \bar{\Psi}\Gamma\lambda_\alpha\Psi$, using the Wilson/clover fermions and Symanzik improved gluons. Extending a calculation up to $\mathcal{O}(a^2)$ brings in new difficulties, compared to lower order in a ; for instance, there appear new types of singularities. The procedure to address this issue is extensively described in Ref. [3]. The $\mathcal{O}(a^2)$ terms of such perturbative computations are of great utility since they can be subtracted from non-perturbative estimates to minimize their lattice artifacts.

The generalized parton distributions (GPDs) of the nucleon determine non-forward matrix elements of gauge invariant light cone operators; the moments of such operators can be evaluated on the lattice. GPDs also give information on interesting quantities such as the quark orbital angular momentum contribution to proton spin [4]. Moreover, the generalized parton distributions can be measured in high energy scattering experiments, for instance the deeply virtual Compton scattering of virtual photons off a nucleon. Thus, by computing moments of GPDs in lattice QCD one can explore many aspects of the nucleon structure. The operators that are related to the GPDs must be renormalized, before one compares results from simulations to physical, experimentally measurable quantities.

In this work, we investigate the perturbative renormalization of the fermion propagator, local and twist-2 fermion operators. We compute all matrix elements for the amputated Green's functions of the inverse fermion propagator, ultralocal bilinears and twist-2 one-derivative operators, defined as $\bar{\Psi}\Gamma_{\{\mu}\overleftrightarrow{D}_{\nu\}}\tau^\alpha\Psi$ (symmetrized and traceless). Although our expressions for all these matrix elements are as general as possible (the dependence on almost all parameters is shown explicitly), these are extremely lengthy and complicated to be presented here. Thus, we show our results only for the renormalization constants and for particular choices of the various parameters. In Section 2 we briefly describe the procedure for these computations and in Sections 3 - 4 we present our results for the renormalization functions. We also compare with non-perturbative estimates provided by the ETM Collaboration. Due to space limitations the renormalization of the ultralocal operators is not discussed here, but will appear in a longer write-up.

2. Description of the calculation

In the framework of this computation we employ a fermion action which includes the clover term, and also an additional mass parameter, μ

$$S_F = \sum_f \sum_x \bar{\Psi}_f(x) \left[\frac{\gamma_\nu}{2} (\nabla_\nu + \nabla_\nu^*) - \frac{ar}{2} \nabla_\nu^* \nabla_\nu + m + i\mu\gamma_5\tau^3 - \frac{1}{4} c_{\text{SW}} \sigma_{\rho\nu} \hat{F}_{\rho\nu}(x) \right] \Psi_f(x) \quad (2.1)$$

A summation over the Dirac indices ν, ρ is implied. The advantage of the above action is that it combines different actions that are used widely: Wilson ($c_{\text{SW}} \rightarrow 0, \mu \rightarrow 0$), clover ($\mu \rightarrow 0$) and twisted mass ($c_{\text{SW}} \rightarrow 0$). It is important to mention that for the case of twisted mass fermions, Eq. (2.1) corresponds to the twisted mass action in the so called twisted basis χ ($\chi = e^{-i\frac{\theta}{2}\gamma_5\tau^3}\Psi$). The appropriate form of this action in physical basis has a rotation of the Wilson term, $r \rightarrow -ir\gamma_5\tau^3$. This is crucial because the definition of the Z -factors in physical and twisted bases are different, for instance $Z_A^{\text{phys}} = Z_V^{\text{twisted}}$ and $Z_V^{\text{phys}} = Z_A^{\text{twisted}}$, for the axial and vector currents with or without a derivative. The results presented here are all in the physical basis.

For the gluon part we use a family of Symanzik improved gluons and more precisely 10 different sets of Symanzik parameters that are widely used in simulations; these are shown in Table 1 of Ref. [3]. In the same reference, the reader can find all details for the calculation procedure and the evaluation of the superficially divergent integrals. The substantial difference with our previous computations is the presence of masses, m and μ , in the fermion propagators. The dependence of superficially divergent integrals on p, m, μ is nontrivial and it is a rather complicated task to extract this dependence explicitly. In fact, there are 11 "strongly" IR divergent integrals (they are convergent only at $D > 6$ dimensions) and a few hundred of divergent integrals at $D = 4 - 2\epsilon$ dimensions.

The 1-loop diagrams that enter our three calculations are shown in Fig. 1. Diagrams 1a and 1b regard the correction to the inverse fermion propagator, diagram 2 corrects the local bilinears and finally diagrams 3a-3d contribute to the calculation of the twist-2 bilinears. The appropriate operator employed in each computation is represented by a cross in diagrams 2, 3a-3d.

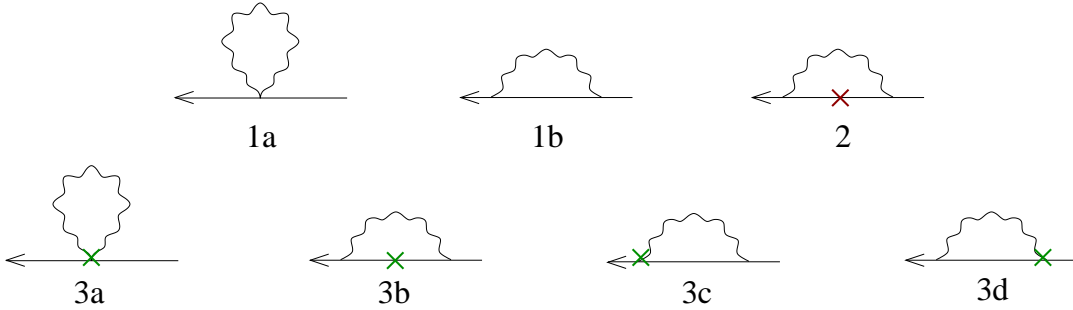


Figure 1: One-loop diagrams contributing to the correction of the amputated Green's functions of the propagator (1a, 1b), local bilinears (2) and twist-2 operators (3a-3d). A wavy (solid) line represents gluons (fermions). A cross denotes an insertion of the operator under study.

3. Renormalization of the fermion field to $\mathcal{O}(a^2)$

For all the renormalization factors used here we employ the RI'-MOM scheme. The fermion field renormalization constant, Z_q , can be obtained using alternative renormalization conditions that differ in their lattice artifacts. The most widely used conditions are the following two

$$Z_q^A = \frac{1}{4} \text{Tr} \left[S_{\text{cont}}(p) \cdot S_{1\text{-loop}}^{-1}(p) \right] \Bigg|_{p^2=\bar{\mu}^2}, \quad S_{\text{cont}}(p) = \frac{-i \sum_{\rho} p_{\rho} \gamma_{\rho}}{p^2} \quad (3.1)$$

$$Z_q^B = \frac{1}{4} \text{Tr} \left[S_{\text{tree}}(p) \cdot S_{1\text{-loop}}^{-1}(p) \right] \Bigg|_{p^2=\bar{\mu}^2}, \quad S_{\text{tree}}(p) = \frac{-i \sum_{\rho} \frac{1}{a} \sin(a p_{\rho}) \gamma_{\rho}}{\frac{1}{a^2} \sum_{\rho} \sin^2(a p_{\rho})} \quad (3.2)$$

with the trace taken over the Dirac indices. The $S_{1\text{-loop}}^{-1}(p)$ is the amputated Green's function for the inverse propagator up to 1-loop; it was computed from diagrams 1a and 1b of Fig. 1. Indeed, the constants Z_q^A and Z_q^B differ only in their lattice artifacts, since the $\mathcal{O}(a^2)$ expansion of $S_{\text{tree}}(p)$ is simply $S_{\text{cont}}(p) + i a^2 \sum_\rho p_\rho^3 \gamma_\rho / (6 p^2)$.

In the most general expression for Z_q , we show explicitly the dependence on the action parameter c_{SW} , the coupling constant g , the number of colors N_c , the gauge fixing parameter λ , the masses m, μ , the lattice spacing a and the external momentum p . On the contrary, we cannot express Z_q in a closed form as a function of the Symanzik parameters, c_0, c_1, c_2, c_3 ; we have computed Z_q for each of the 10 sets of Symanzik coefficients shown in Table 1 of Ref. [3]. Next we provide our result for Z_q using the condition in Eq. (3.1), for the Landau gauge, $c_{\text{SW}} = 0$, $m = 0$ and tree-level Symanzik improved gluons

$$\begin{aligned}
 Z_q^A = & \left[1 - \frac{a^2 p^4}{6 p^2} + \frac{C_F g^2}{16 \pi^2} \left\{ -13.0232726(2) + a^2 \left(-\ln[a^2 \mu^2 + a^2 p^2] \left(\frac{2}{3} \mu^2 + \frac{73}{360} p^2 + \frac{157}{180} \frac{p^4}{p^2} \right) \right. \right. \\
 & + 1.1590439(1) \mu^2 + 4.2770447(3) \frac{p^4}{p^2} + 1.1471634(1) p^2 + \frac{7}{40} \frac{\mu^8}{(p^2)^3} \\
 & - \frac{1}{240} \frac{\mu^6}{(p^2)^2} - \frac{37}{180} \frac{\mu^4}{p^2} - \frac{7}{20} \frac{\mu^8 p^4}{(p^2)^5} + \frac{1}{120} \frac{\mu^6 p^4}{(p^2)^4} + \frac{169}{180} \frac{\mu^4 p^4}{(p^2)^3} - \frac{43}{80} \frac{\mu^2 p^4}{(p^2)^2} \\
 & + \ln \left[1 + \frac{p^2}{\mu^2} \right] \left(-\frac{7}{40} \frac{\mu^{10}}{(p^2)^4} - \frac{1}{12} \frac{\mu^8}{(p^2)^3} + \frac{2}{9} \frac{\mu^6}{(p^2)^2} - \frac{1}{3} \frac{\mu^4}{p^2} \right. \\
 & \left. \left. + \frac{7}{20} \frac{\mu^{10} p^4}{(p^2)^6} + \frac{1}{6} \frac{\mu^8 p^4}{(p^2)^5} - \frac{35}{36} \frac{\mu^6 p^4}{(p^2)^4} + \frac{1}{12} \frac{\mu^4 p^4}{(p^2)^3} \right) \right] \Bigg|_{p^2 = \bar{\mu}^2} \quad (3.3)
 \end{aligned}$$

In the above expression $p^4 \equiv \sum_\nu p_\nu^4$, $C_F = (N_c^2 - 1)/(2N_c)$, and $\bar{\mu}$ is the renormalization scale. No $\mathcal{O}(a^1)$ terms appear in Eq. (3.3) since we set m equal to zero. Although the mass dependence shown in Eq. (3.3) is very complicated, the numerical result for the renormalization constant Z_q depends mildly on μ (for the values used in numerical simulations by ETMC, $0.003 \leq \mu \leq 0.01$).

A very important issue is that the $\mathcal{O}(a^2)$ terms depend not only on p^2 , but also on the direction of the momentum p , as manifested by the presence of p^4 . As a consequence, different renormalization prescriptions, involving the same renormalization scale $\bar{\mu}$ but different directions of p , lead to a different renormalization constant. The strategy one may follow is to average over the results for Z_q which are obtained using these different directions.

In Table 1 we present our 1-loop results for Z_q , up to $\mathcal{O}(a^2)$, for the two renormalization conditions: Eq. (3.1) (Z_q^A) and Eq. (3.2) (Z_q^B). The results are given in the chiral limit for the Landau gauge, $c_{\text{SW}} = 0$, $N_c = 3$ and for 3 values of the coupling constant $\beta = 2N_c/g^2$. Instead of the bare coupling we have used the tadpole-improved coupling [6], defined as $g_t^2 = g^2 / \langle plaq \rangle$, to achieve further improvement. The renormalization scale $\bar{\mu}$ was set to $1/a$, that is $a^2 p^2 = 1$. This is a well-defined choice, since all possible lattice momenta (permutations of $(\pm 1, 0, 0, 0)$) have the same p^4 . Thus, Z_q is the same for all these permutations. $Z_q^{A \mathcal{O}(a^2)}$ and $Z_q^{B \mathcal{O}(a^2)}$ are the $\mathcal{O}(a^2)$ effects of Z_q^A and Z_q^B respectively. The last column gives the non-perturbative estimates of ETMC [5], using the renormalization condition of Eq. (3.2) and employing the same parameters as we did. In $Z_q^{\text{non-pert}}$ our $\mathcal{O}(a^2)$ corrections were already subtracted to reduce lattice artifacts. In fact, ETMC applied the subtraction procedure to all their data; therefore, the behavior of $Z_q^{\text{non-pert}}$ against the

renormalization scale becomes flatter in the energy region where perturbation theory is valid. This indicates that the lattice artifacts are suppressed.

β	Z_q^A	$Z_q^A \mathcal{O}(a^2)$	Z_q^B	$Z_q^B \mathcal{O}(a^2)$	$Z_q^{non-pert}$
3.80	0.655255014(4)	-0.039554503(1)	0.771056601(4)	0.076247083(1)	0.755(4)
3.90	0.663871997(4)	-0.045705298(1)	0.782134880(4)	0.072557584(1)	0.757(3)
4.05	0.675276827(4)	-0.053846057(1)	0.796797308(3)	0.067674424(1)	0.777(5)

Table 1: Perturbative and non-perturbative estimates of Z_q for different coupling constants, in the chiral limit and using two renormalization conditions, for tree-level Symanzik gluons, $c_{sw} = 0$, $N_c = 3$.

The numbers in parenthesis denote the systematic errors coming from our procedures for numerical integration over loop momenta. Since we have used two alternative renormalization conditions, it is worth comparing their lattice artifacts. For $\bar{\mu}^2 = 4$ and the same parameters of Table 1, we isolated the contribution of the $\mathcal{O}(a^2)$ terms and tabulated them in Table 2. In the same Table we present the averaged results, $\langle Z_q^A \mathcal{O}(a^2) \rangle$, $\langle Z_q^B \mathcal{O}(a^2) \rangle$. For the averaging we used all 24 lattice momenta with $a^2 p^2 = 4$: 16 permutations of $(\pm 1, \pm 1, \pm 1, \pm 1)$ and 8 permutations of $(\pm 2, 0, 0, 0)$. One observes that, although the condition in Eq. (3.1) gives $\mathcal{O}(a^2)$ correction at tree level for Z_q^A , the combined $\mathcal{O}(a^2)$ effects in Z_q^A are much smaller than the ones of Z_q^B , which is exactly 1 at tree level. It is also evident that averaging over momenta with different directions helps to reduce the overall $\mathcal{O}(a^2)$ contributions.

β	$Z_q^A \mathcal{O}(a^2)$	$\langle Z_q^A \mathcal{O}(a^2) \rangle$	$Z_q^B \mathcal{O}(a^2)$	$\langle Z_q^B \mathcal{O}(a^2) \rangle$
3.80	0.35679267(9)	0.29105315(4)	0.45876742(9)	0.34204053(4)
3.90	0.26014128(8)	0.23208860(4)	0.41544327(8)	0.30973960(4)
4.05	0.13958988(7)	0.15854326(3)	0.36140590(7)	0.26945127(3)

Table 2: The $\mathcal{O}(a^2)$ contributions up to 1-loop in the perturbative results for the Z_q at $\bar{\mu}^2 = 4$.

4. $\mathcal{O}(a^2)$ corrections to the renormalization of twist-2 fermion bilinears

In this section we present the computation of the amputated Green's functions for the following two twist-2 operators

$$\mathcal{O}_V^{\{v_1, v_2\}} = \frac{1}{2} \left[\bar{\Psi} \gamma_{v_1} \overleftrightarrow{D}_{v_2} \tau^\alpha \Psi + \bar{\Psi} \gamma_{v_2} \overleftrightarrow{D}_{v_1} \tau^\alpha \Psi \right] - \frac{1}{4} \delta_{v_1 v_2} \sum_\rho \bar{\Psi} \gamma_\rho \overleftrightarrow{D}_\rho \tau^\alpha \Psi \quad (4.1)$$

$$\mathcal{O}_A^{\{v_1, v_2\}} = \frac{1}{2} \left[\bar{\Psi} \gamma_5 \gamma_{v_1} \overleftrightarrow{D}_{v_2} \tau^\alpha \Psi + \bar{\Psi} \gamma_5 \gamma_{v_2} \overleftrightarrow{D}_{v_1} \tau^\alpha \Psi \right] - \frac{1}{4} \delta_{v_1 v_2} \sum_\rho \bar{\Psi} \gamma_\rho \overleftrightarrow{D}_\rho \tau^\alpha \Psi \quad (4.2)$$

which are symmetrized and traceless, to avoid mixing with lower dimension operators. We have computed, to $\mathcal{O}(a^2)$, the matrix elements of these operators for general external indices v_1, v_2 , mass, g, N_c, a, p, c_{sw} and λ . The final results are available for the 10 sets of Symanzik coefficients we have used in the calculation of Z_q .

The one-derivative operators fall into two different irreducible representations of the hypercubic group, depending on the choice of the external indices v_1, v_2 . Hence, we distinguish between

$$Z_V^1 \equiv Z_V^{v_1=v_2}, \quad Z_V^2 \equiv Z_V^{v_1 \neq v_2}, \quad Z_A^1 \equiv Z_A^{v_1=v_2}, \quad Z_A^2 \equiv Z_A^{v_1 \neq v_2} \quad (4.3)$$

The renormalization conditions from which Z_V and Z_A are obtained, is defined in the RI'-MOM scheme, as

$$Z_q^{-1} Z_{\mathcal{O}}^{v_1 v_2} \text{Tr} \left[\Lambda_{\mathcal{O}}^{v_1 v_2}(p) \cdot \Lambda_{\mathcal{O} \text{ cont}}^{v_1 v_2} \right] \Bigg|_{p^2=\bar{\mu}^2} = \text{Tr} \left[\Lambda_{\mathcal{O} \text{ cont}}^{v_1 v_2} \cdot \Lambda_{\mathcal{O}}^{v_1 v_2} \right] \Bigg|_{p^2=\bar{\mu}^2}, \quad \Lambda_{\mathcal{O} \text{ cont}}^{v_1 v_2} = i\Gamma_{\{v_1 p \mu_2\}} - \text{traces} \quad (4.4)$$

where $\Gamma_{v_1} = \gamma_{v_1}, \not{v}_1 \gamma_{v_1}$. The quantity $\Lambda_{\mathcal{O}}^{v_1 v_2}(p)$ is our result up to 1-loop for the amputated Green's function for each operator. In the renormalization condition there is a choice of using $\Lambda_{\mathcal{O} \text{ tree}}^{v_1 v_2}$ instead of $\Lambda_{\mathcal{O} \text{ cont}}^{v_1 v_2}$. The final Z-factors of the two choices have different lattice artifacts. Applying the renormalization condition and using the Z_q that we computed perturbatively with its $\mathcal{O}(a^2)$ corrections, we have the results for Z_V and Z_A . In Table 3 we present these results in the chiral limit, for tree-level Symanzik gluons, $\beta = 3.9$, $c_{\text{SW}} = 0$ and Landau gauge. We chose six different values of the momentum, thus six renormalization scales. For Z_q we employed Eq. (3.1), and we used $\Lambda_{\mathcal{O} \text{ cont}}^{v_1 v_2}$ in Eq. (4.4). The extrapolation errors are smaller than the last digit shown in Table 3.

ap	Z_V^1	Z_V^2	Z_A^1	Z_A^2
(4,2,2,2)	1.04129	1.05738	1.08270	1.06309
(5,2,2,2)	1.04411	1.04331	1.08772	1.04669
(6,2,2,2)	1.04881	1.02365	1.09312	1.02496
(3,3,3,3)	1.00343	1.05427	1.03778	1.03607
(4,3,3,3)	0.99660	1.05237	1.04456	1.03289
(5,3,3,3)	0.99731	1.04736	1.05543	1.02660

Table 3: Perturbative results for Z_A and Z_V in the chiral limit, for various renormalization scales. The action parameters are: tree-level Symanzik gluons, Landau gauge, $\beta = 3.9$, $c_{\text{SW}} = 0$, $N_c = 3$.

For the case of the vector operator with $v_1 \neq v_2$ we give the result for $\text{Tr} \left[\Lambda_V^{v_1 v_2}(p) \cdot \Lambda_{\mathcal{O} \text{ cont}}^{v_1 v_2} \right]$ which contributes to Z_V^2 , for the Landau gauge, tree-level Symanzik gluons, $c_{\text{SW}} = 0$, $\mu = 0$

$$\begin{aligned} \text{Tr} \left[\Lambda_V^{v_1 v_2}(p) \cdot \Lambda_{\mathcal{O} \text{ cont}}^{v_1 v_2} \right] &= -p_{v_1}^2 - p_{v_2}^2 + a^2 \frac{p_{v_1}^4 + p_{v_2}^4}{6} + \frac{C_F g^2}{16\pi^2} \left[15.045752(1) p_{v_1}^2 + \frac{4 p_{v_1}^2 p_{v_2}^2}{3 p^2} \right. \\ &\quad - \frac{8 p_{v_1}^2 \ln(p^2)}{3} + a^2 \left(-0.13212(3) p^2 p_{v_1}^2 - 4.6352(1) p_{v_1}^4 - 4.0096(1) p_{v_1}^2 p_{v_2}^2 \right. \\ &\quad + \frac{353}{720} \frac{p^4 p_{v_1}^2}{p^2} + \frac{29}{90} \frac{p^4 p_{v_1}^2 p_{v_2}^2}{(p^2)^2} + \frac{179}{90} \frac{(p_{v_1}^4 p_{v_2}^2 + p_{v_1}^2 p_{v_2}^4)}{p^2} \\ &\quad \left. \left. + \ln(a^2 p^2) \left(-\frac{103}{360} p^2 p_{v_1}^2 + \frac{331}{360} p_{v_1}^4 + \frac{1013}{180} p_{v_1}^2 p_{v_2}^2 \right) \right) \right] \\ &\quad + \text{symmetric terms : } v_1 \leftrightarrow v_2 \quad (4.5) \end{aligned}$$

It is now interesting to use non-perturbative estimates for Z_A and Z_V , combined with our $\mathcal{O}(a^2)$ terms, in order to see if the subtraction procedure works well for these operators. Our collaborators in ETMC provided us with data for the physical Z_A^2 [7] corresponding to the six momenta of Table 3. Note that the momenta can be grouped into two categories, according to their spatial values: (2,2,2) or (3,3,3). Non-perturbatively it is observed that these groups have different lattice artifacts and a discontinuity appears in the Z -factors with one derivative, as shown in Fig. 2. We also plot the subtracted non-perturbative data, which exhibit a smooth behavior of Z_A^2 . The errors are too small to be visible.

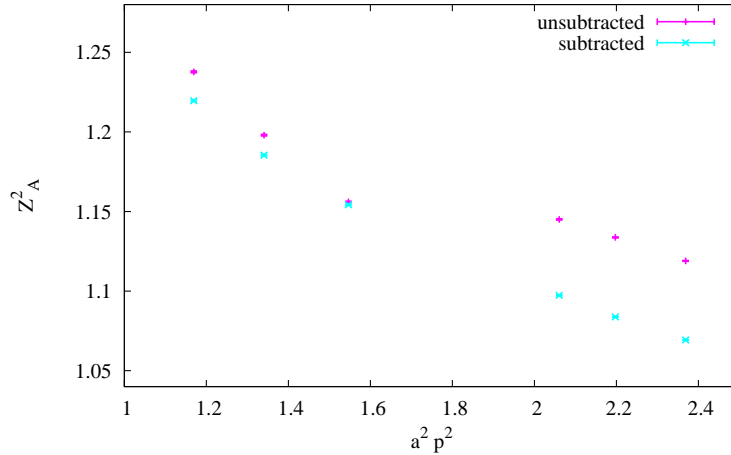


Figure 2: Physical non-perturbative Z_A^2 with subtractions of $\mathcal{O}(a^2)$ terms.

Another plot demonstrating the achieved improvement of non-perturbative estimates for the renormalization constants using our a^2 correction terms, is shown in Ref. [8]. In particular, for the local axial renormalization constant it is shown that, by converting the subtracted numbers into \overline{MS} scheme and setting the renormalization scale to 2GeV, one obtains a good plateau when plotting Z_A for each of the momentum 4-vectors.

References

- [1] K. Symanzik, *Continuum limit and improved action in lattice theories*, *Nucl. Phys.* **B226** (1983) 187; *Nucl. Phys.* **B226** (1983) 205.
- [2] R. Frezzotti, P. Grassi, S. Sint, P. Weisz, *Lattice QCD with a chirally twisted mass term*, *JHEP* **08** (2001) 058, [hep-lat/0101001].
- [3] M. Constantinou, V. Lubicz, H. Panagopoulos, F. Stylianou, *$\mathcal{O}(a^2)$ corrections to the one-loop propagator and bilinears of clover fermions with Symanzik improved gluons*, *JHEP*, to appear, [arXiv:0907.0381].
- [4] X. Ji, *Gauge-Invariant Decomposition of Nucleon Spin and Its Spin-Off*, *Phys. Rev. Lett.* **78** (1997) 610, [hep-ph/9603249].
- [5] ETM Collaboration, in preparation.
- [6] G. Lepage and P. Mackenzie, *On the Viability of Lattice Perturbation Theory*, *Phys. Rev.* **D48** (1993) 2250, [hep-lat/9209022].
- [7] C. Alexandrou, M. Constantinou, T. Korzec, in preparation.
- [8] C. Alexandrou, M. Constantinou, T. Korzec, *Generalized Parton Distributions of the Nucleon from twisted mass QCD*, *POs (LAT2009)* 136.